Surface diffusion of a glassy discotic organic semiconductor

Yuhui Li[1], Camille Bishop[2], Kai Cui[2], J. R. Schmidt[2], M. D. Ediger[2], Lian Yu[1*]

[1] School of Pharmacy, University of Wisconsin-Madison, Madison, WI, 53705, USA

[2] Department of Chemistry, University of Wisconsin-Madison, Madison, WI, 53706, USA

Abstract. Surface diffusion has been measured in the glass of an organic semiconductor, MTDATA, using the method of surface grating decay. The decay rate was measured as a function of temperature and grating wavelength, and the results indicate that the decay mechanism is viscous flow at high temperatures and surface diffusion at low temperatures. Surface diffusion in MTDATA is enhanced by 4 orders of magnitude relative to the bulk rate when compared at T_g. The result on MTDATA has been analyzed along with the results on other molecular glasses without extensive hydrogen bonds. In total, these systems cover a wide range of molecular geometries from rod-like to quasi-spherical to discotic and their surface diffusion coefficients vary by 9 orders of magnitude. We find that the variation is well explained by the existence of a steep surface mobility gradient and the anchoring of surface molecules at different depths. Quantitative analysis of these results supports a recently proposed double-exponential form for the mobility gradient: $\log D(T, z) = \log D_v(T) + [\log D_0 - \log D_v(T)] \exp(-z / \xi)$, where $D(T, z)$ is the depth-dependent diffusion coefficient, $D_v(T)$ is the bulk diffusion coefficient, $D_0 \approx 10^{-8}$ m^2/s, and $\xi \approx 1.5$ nm. Assuming a representative bulk diffusion coefficient for fragile glass formers, it reproduces the presently known surface diffusion rates within 0.6 decade. Our result is relevant for predicting the surface diffusion rates in molecular glasses.

Introduction

Molecules at the surface of a liquid or glass experience a different environment from those in the bulk and as a result, can have different packing arrangements and dynamics.[1,2,3] The surface dynamics of glasses plays a key role in their stability and fabrication; for example, surface mobility enables fast local crystal growth,[4,5] preparation of ultra-stable glasses by physical vapor deposition,[6,7] transformation of nanostructures,[8,9] and cold welding.[10]

The substance of this study, 4,4',4''-Tris[(3-methylphenyl)phenylamino]triphenylamine (MTDATA, Scheme 1), exemplifies a discotic "starburst" molecule synthesized as a hole-transport material in organic light-emitting diodes (OLEDs).[11,12,13,14] Given that active layers in OLEDs are often amorphous films prepared by physical vapor deposition (PVD), understanding the surface dynamics during deposition helps control film structure and device performance.[15,16] Efficient surface equilibration enables the preparation of high-density, high-stability glass films[17] with controlled anisotropic packing.[18] In this work, we investigate the surface diffusion of MTDATA, an important measure of its surface mobility.

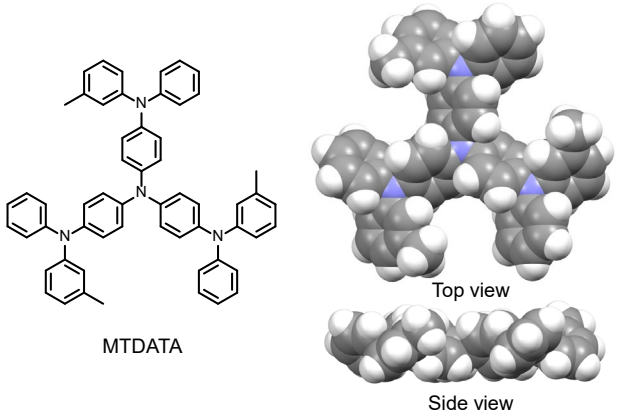

Scheme 1. Molecular structure of MTDATA. On the right are DFT optimized structures in top and side views.

Apart from its importance in organic electronics, MTDATA is relevant for understanding surface diffusion. Previous work has observed a large variation of the surface diffusion coefficient D_s between materials.[19] For molecular glasses without extensive hydrogen bonds (e.g., MTDATA), Li et al. observed that the variation of D_s correlates with the depth of penetration of surface molecules.[20] That is, the deeper a molecule penetrates into the bulk, the lower its surface diffusion rate. This is attributed to the existence of a steep mobility gradient beneath the surface and argued that lateral diffusion of a molecule is essentially limited by its deepest part where mobility is lowest. The collection of molecules on which their conclusion is based has quasi-spherical, chain-like, and rod-like geometries, but no discotic molecules like MTDATA. Here we test the conclusion for a discotic molecule. In addition, we examine the depth profile of surface mobility using all available data across all measurement temperatures.

We report that surface diffusion in an MTDATA glass significantly outpaces bulk diffusion, by approximately 4 orders of magnitude when compared at T_g. Despite this new discotic geometry, the MTDATA result is fully consistent with the previous conclusion that the depth of penetration controls the lateral diffusion of molecules at the liquid/vapor interface. We show that all the molecular glasses studied to date without extensive hydrogen bonds are characterized by a similar surface mobility gradient. The depth profile of this mobility gradient has the double-exponential form observed by simulations[21,22] and we use the available surface-diffusion data to determine the parameters that characterize the mobility gradient.

Experimental Section

4,4',4"-Tris[(3-methylphenyl)phenylamino]triphenylamine (MTDATA, sublimed, purity > 98%) was obtained from Ossila and used as received. T_g of MTDATA was determined by the onset of glass transition during 10 K/min heating using Differential Scanning Calorimetry (DSC, TA Q2000). To make a surface grating, a master pattern was placed on a viscous liquid of MTDATA at 388 K. The master was removed after vitrifying the liquid at 323 K, producing a corrugated surface. Master gratings of different wavelengths were purchased or fabricated. For λ = 1000 nm and 1984 nm, plastic gratings were purchased from Rainbow Symphony; for λ = 334 nm and 729 nm, the masters were duplicated from a Blu-ray or DVD disc through a UV-curing polymer (Norland Optical Adhesive 61); for λ = 424 and 3322 nm, the masters were duplicated from a glass grating (Spectrum Scientific) through the same transfer process. All masters were coated with 10 nm gold before use (Sputter Deposition System, Leica ACE600) to minimize contamination during subsequent use. The thickness of each embossed MTDATA glass film was 50 – 100 μm, much larger than the wavelength of any surface grating used, ensuring that the evolution of the top surface was unaffected by the substrate.

The evolution of a surface grating was measured by either Atomic Force Microscopy (AFM, Bruker Veeco Multiple Mode IV) or laser diffraction. AFM was performed in the tapping mode; the amplitude h of the sinusoidal surface was obtained by Fourier transforming the height profile. Laser diffraction was used to determine faster decays than feasible with AFM. A HeNe laser (λ = 632.8 nm, Uniphase Corp.) passed through a surface grating sample in a transmission geometry and the first-order diffraction was captured by a silicon amplified detector (Thorlabs) interfacing with a National Instruments LabVIEW program. The two methods yielded identical results within experimental error when applied to the same decay

process. During grating decay, the sample was purged with dry nitrogen and its temperature was controlled within 0.1 K with a Linkam microscope temperature stage or a custom-made mini-oven.

Density functional theory (DFT) calculations were performed in Molpro 2015 software[23] through the ASE interface[24], using the Perdew-Burke-Ernzerhof exchange-correlation functional[25] combined with DFT-D3 dispersion correction.[26] Dunning style aug-cc-pVDZ basis sets[27] were used. Geometry of the molecule was relaxed until maximum force on atoms was less than 0.01 eV/A.

Results

The method of surface grating decay was used to investigate the surface diffusion in amorphous MTDATA. Figure 1 shows the typical decay kinetics recorded by laser diffraction (Figure 1a) and by AFM (Figure 1b). Laser diffraction was used to measure fast decays at high temperatures and AFM to measure slow decays at low temperatures. We observed exponential decays. The decay constant K was obtained by fitting the grating amplitude h from AFM to the function $h = h_0 \exp(-Kt)$ and the diffraction intensity I to $(I/I_0)^{1/2} = \exp(-Kt)$, accounting for the fact that $I \propto h^2$. The decay constant is plotted in Figure 2 as a function of temperature for λ = 334 nm.

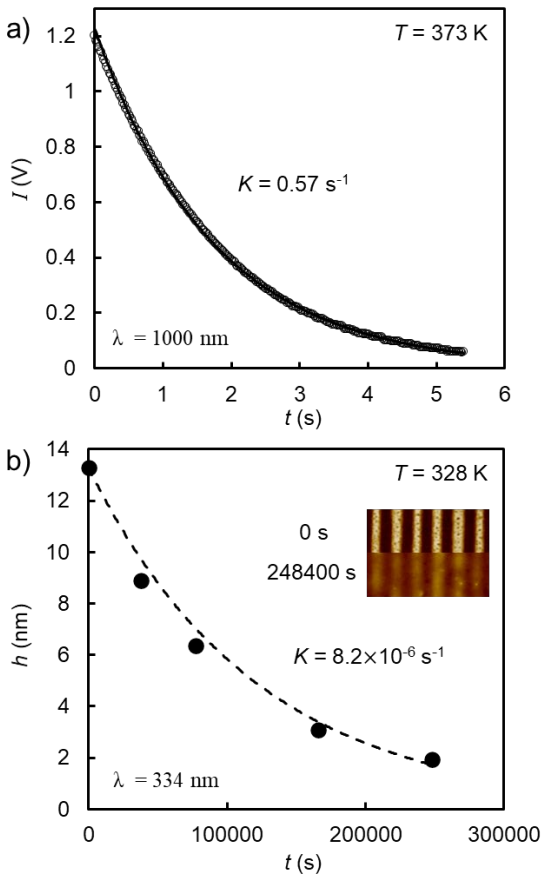

Figure 1. Decay kinetics of MTDATA surface gratings. (a) At 373 K, recorded by laser diffraction (λ = 1000 nm). (b) At 328 K, recorded by AFM (λ = 334 nm). Inset: AFM images at two time points.

According to Mullins,[28] the amplitude h of a sinusoidal surface contour decreases exponentially over time, $h = h_0 \exp(-Kt)$, and the decay rate K is given by:

$$K = Fq + Aq^2 + (A' + C)q^3 + Bq^4 \qquad (1)$$

In eq. 1, $q = 2\pi/\lambda$, where λ is the wavelength of the grating, and the different terms correspond to the different mechanisms of surface evolution: viscous flow (the F term), evaporation-condensation (A and

113 *A*'), bulk diffusion (*C*), and surface diffusion (*B*). Among
114 these, viscous flow and surface diffusion are the
115 dominant mechanisms for surface evolution of molecular
116 glasses near T_g.[1,20] These two terms are given by: $F = \gamma/2\eta$ and $B = D_s\gamma\Omega^2\nu/(kT)$, where γ is the surface tension,
118 η the viscosity, D_s the surface diffusion coefficient, Ω
119 the molecular volume, ν the areal density of surface
120 molecules, and k the Boltzmann constant.

121

122 Figure 2 shows that the decay constant K has stronger
123 temperature dependence at high temperature than at low
124 temperatures and the transition occurs around the DSC T_g
125 (vertical line). To determine the mechanism of surface
126 evolution, we measured the wavelength dependence of K.
127 According to Mullins (eq. 1), viscous relaxation of a
128 surface is characterized by $K \propto \lambda^{-1}$, whereas flattening by
129 surface diffusion by $K \propto \lambda^{-4}$. Figure 3 shows the
130 wavelength dependence of K at 363 K and 343 K, with
131 363 K falling in the high-temperature region of Figure 2
132 and 343 K in the low-temperature region. At 363 K, we
133 observe $K \propto \lambda^{-1.1}$, and at 343 K, $K \propto \lambda^{-3.7}$. Thus the
134 wavelength test verifies a change of decay mechanism
135 from viscous flow at high temperatures to surface
136 diffusion at low temperatures.

137

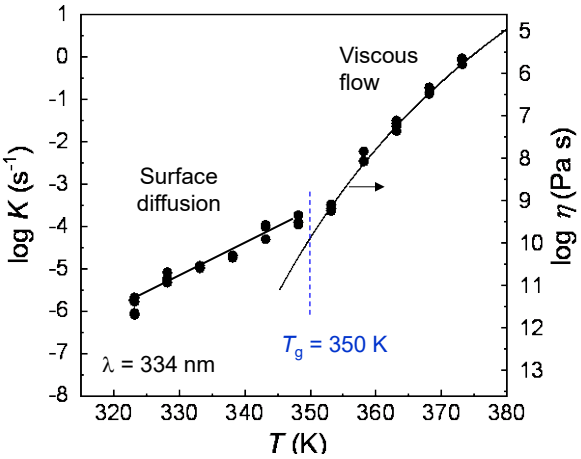

Figure 2. Grating decay constant K plotted against temperature. Viscosity is calculated from the decay constant and shown using the second y axis.

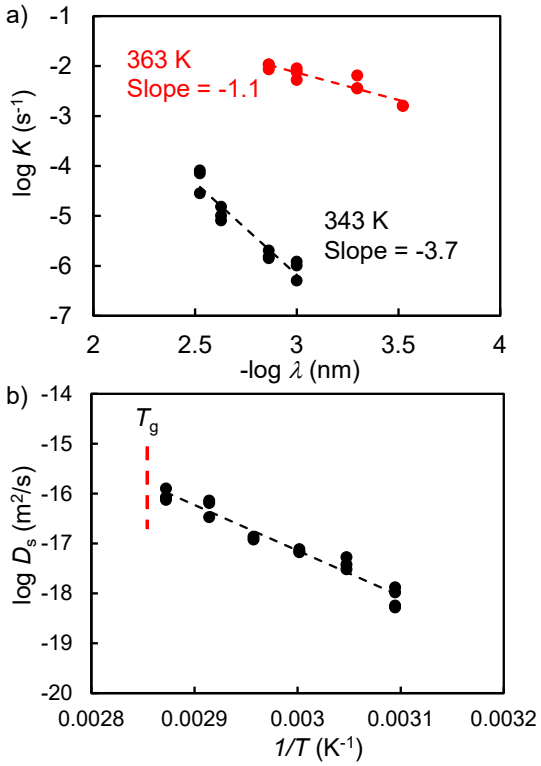

Figure 3. (a) Grating decay constants plotted against wavelength of the surface gratings. (b) Surface diffusion rate as a function of temperature.

138 As a further test of viscous flow as the high-temperature
139 decay mechanism, we calculate the viscosity of
140 MTDATA from the decay constant above 353 K. For this decay mechanism, $K = Fq = \pi\gamma/(\lambda\eta)$, yielding
141 $\eta = \pi\gamma/\lambda K$. The calculated viscosity is shown in Figure 2 using the second y axis. In this calculation, we

assume $\gamma = 0.05$ N/m, a typical value for the surface tension of organic liquids. The upper curve in Figure 2 is a fit of the calculated viscosity to the Vogel-Fulcher-Tammann (VFT) equation, $\log \eta = A + B / (T - T_0)$. This function is known to provide an accurate description of the temperature dependence of viscosity. Thus the quality of the VFT fit supports the assignment of viscous flow as the decay mechanism. When extrapolated to low temperatures, the VFT curve is below the observed decay constants, signaling the activation of a faster decay mechanism (surface diffusion). From the extrapolation, we obtain $\eta_g = 10^{10}$ Pa s at the DSC T_g (350 K), in agreement with the typical values for organic liquids;[29] for example, $\eta_g = 10^{9.9}$ Pa s for OTP[30] and $10^{9.5}$ Pa s for TNB.[31] In addition, we obtain the fragility of MTDATA, $m = 85$, a typical value for organic liquids.

From the decay constant at low temperatures, we calculate the surface diffusion coefficient D_s of MTDATA (eq. 1) and the results are shown in Figure 3b. For this calculation, we assume $\gamma = 0.05$ N/m. $\Omega = 1.09$ nm^3 is obtained by the bulk density (assumed to be 1.20 g/cm^3) and molecular weight (789.2 g/mol), and ν is obtained from $\nu = \Omega^{-2/3} = 0.94$/nm^2. In the temperature range of study, surface diffusion has an Arrhenius kinetics with an activation energy of $E_a = 175$ kJ/mol.

Figure 4 compares the D_s values of MTDATA and other molecular glasses: *ortho*-terphenyl (OTP),[32] *tris*-naphthyl benzene (TNB),[33] indomethacin (IMC),[1] polystyrene (PS) oligomers (1110 and 1700 g/mole),[34] and posaconazole (POS).[20] The bulk diffusion coefficients D_v of the same systems are also plotted when available.[35,36,37,38] The temperature has been scaled by T_g and in this format, the D_v values cluster together, while the D_s values are widely different. The D_s of MTDATA is at the low end of the measured D_s values, but still significantly larger than the clustered D_v values, by approximately 4 orders of magnitude

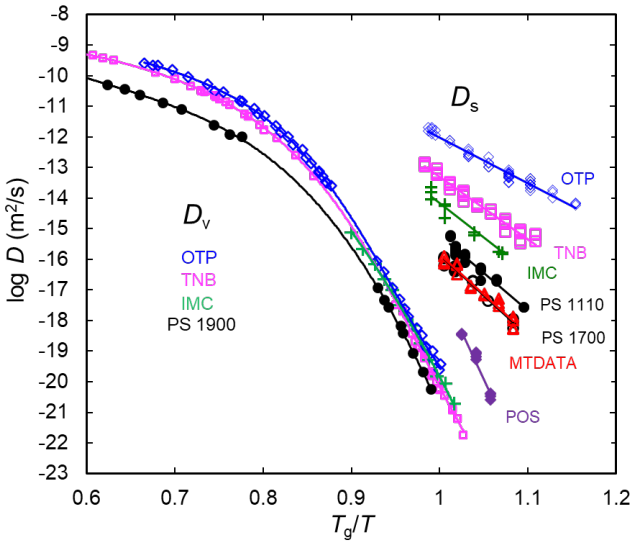

Figure 4. Surface and bulk diffusion coefficients of MTDATA and other organic glasses. T_g is the onset temperature of glass transition measured by DSC during heating at 10 K/min.

when compared at T_g. On this plot, MTDATA and PS 1700 are nearly coincident despite their rather different molecular weights (789 g/mole and 1700 g/mole). As we discuss later, this arises from their similar penetration depths into the bulk glass.

Discussion

We have measured the surface diffusion in the glass of the discotic molecule MTDATA using the method of surface grating decay. Similar to other molecular glasses, surface evolution occurs by viscous flow at high temperatures and by surface diffusion at low temperatures. The low-temperature data allowed calculation of the surface diffusion coefficient of MTDATA (Figure 3b) for comparison with the values of other systems (Figure 4). The surface diffusion of MTDATA is enhanced relative to the typical bulk rate by 4 orders of magnitude when evaluated at T_g. This finding is consistent with the enhanced stability of MTDATA glasses prepared by PVD relative to the ordinary liquid-cooled counterpart.[39] We now discuss the MTDATA result in relation to the other systems investigated and show that the depth of penetration of surface molecules plays a central role in defining the rate of surface diffusion. This allows a quantitative depth profiling of the surface mobility gradient and our result supports double-exponential form recently observed by simulations.

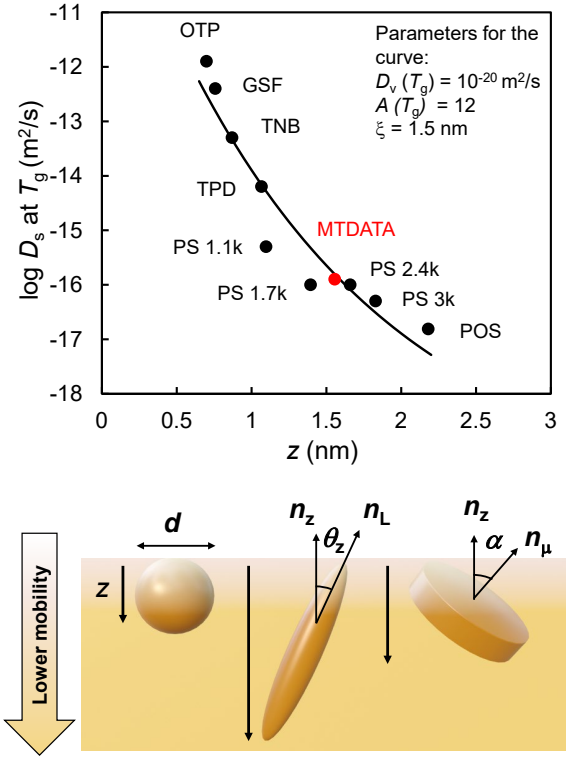

Figure 5. Surface diffusion coefficient D_s at T_g vs. the penetration depth z. The curve is a fit of the data to eq. 2. The calculation of the penetration depth z is illustrated at the bottom for quasi-spherical, rod-like and discotic molecules. $z = d$ for a quasi-spherical molecule, where d is molecular diameter. $z = L \cos \theta_z$ for a rod-like molecule where L is rod length and θ_z the average angle between the long axis and the surface normal. $z = D \sin \alpha$ for a discotic molecule, where D is the disc diameter and α is the average angle between the disc normal and the surface normal.

Li et al. investigated the effect of the penetration depth of surface molecules on the rate of surface diffusion.[20] They plotted the surface diffusion coefficient D_s at T_g as a function of the penetration depth z and observed a downward trend. We reproduce their plot in Figure 5 and add the new MTDATA point. The central idea in this analysis is that a surface molecule can penetrate into the

bulk by one to a few nanometers and according to simulations, local mobility can decrease substantially in this depth range.[22] As a result, the bottom of the molecule would experience a different, lower-mobility environment from the top and it is the bottom of the molecule that determines the rate of the lateral diffusion. By this reasoning, the deeper the penetration, the slower the surface diffusion. Li et al. have treated the calculation of the penetration depths of quasi-spherical and rod-like molecules as illustrated at the bottom of Figure 5. For a discotic molecule like MTDATA, $z = D \sin \alpha$, where D is the disc diameter and α is the average angle between the disc normal and the surface normal. For MTDATA, D = 1.9 nm from DFT calculations. As for the angle α, we recall that the glass film of MTDATA prepared by PVD onto a substrate held near T_g shows no strong molecular orientation.[40] In contrast, significant molecular orientation exists in the glass film of rod-like molecules deposited near T_g, by inheriting the preferred orientation at the interface. We interpret this to mean that MTDATA molecules do not have strongly preferred orientations at the liquid/vapor interface. This interpretation is consistent with the nearly isotropic near-surface orientation of a similar discotic molecule TCTA recently determined by Polarization Resonant Soft X-ray Reflectivity.[41] Thus, we take the average value of α to be 55°, corresponding to random orientation, and obtain z = 1.6 nm. Figure 6 shows that the MTDATA point joins the previously observed trend for other molecular shapes. This result indicates that regardless of the detailed molecular shape, surface diffusion rate is mainly determined by how deeply the molecule penetrates into the bulk.

In Figure 6, the D_s vs penetration depth data have been fitted using a double-exponential function:

$$\log D_s(T) = \log D_v(T) + A(T) \exp(-z/\xi) \qquad (2)$$

This function is inspired by the finding by simulations that near-surface structural relaxation time $\tau(T, z)$ has a double-exponential dependence on depth.[21,22] This form has been rationalized as a consequence of geometric-like, layer-wise transfer of caging constraint.[42,43] In using this form,[20] we follow Ref. 3 and assume that diffusivity is inversely proportional to $\tau(T, z)$ in the mobile surface layer. The physical meaning of eq. 2 is (1) the activation barrier for diffusion increases exponentially with depth, and (2) the surface diffusion rate for a given molecule is determined by its deepest part where mobility is the lowest. In eq. 2, $A(T)$ describes the temperature-dependent difference between surface and bulk mobility, and ξ

describes the rate at which mobility decreases with depth. In this fitting, we fix D_v (T_g) at 10^{-20} m^2/s, a typical value for molecular glasses at T_g (see Figure 4), and obtain: A (T_g) = 12 and ξ = 1.5 nm. In principle, each system in Figure 5 has its own A and ξ values, but the successful fitting of all the data to eq. 2 indicates that these systems are well described by a *common* set of parameters. That is, a similar surface mobility gradient characterizes all these systems. In this mobility gradient (valid for T_g), the diffusion rate decreases by 12 orders of magnitude from the surface ($z = 0$) to the bulk ($z = \infty$), and the activation energy for diffusion increases exponentially with depth with a characteristic length of $\xi = 1.5$ nm. This is a remarkable result given the large differences between these systems in molecular weight (a factor of 10) and shape (quasi-spherical, rod-like, chain-like and discotic). One common feature of these systems is the absence of extensive hydrogen bonding, which has an independent slowing effect on surface diffusion.[19]

Given the success of eq. 2 to describe surface diffusion at T_g, we now explore the possibility to generalize it to *all* temperatures. For this purpose, we recall that the D_s and D_v values for the same system measured at different temperatures follow a power law.[19] In Figure 6, we plot D_s against D_v for the three systems for which both properties have been measured: OTP,[32,35] TNB,[33,36] and IMC. [1,37] For each system, the data are well described by a power law:

$$D_s = D_v^{\,x}\, D_0^{\,1-x} \qquad (3)$$

where x is a coupling constant (0 – 1) and D_0 corresponds to the high-temperature condition at which $D_s = D_v$. For all three systems, $D_0 = 10^{-8}$ m^2/s is consistent with the high-temperature extrapolation of the data, converging at the + sign in Figure 6. For OTP, the validity of eq. 3 and the D_0 value is further supported by simulations performed near $D_v = 10^{-11}$ m^2/s.[44] Eq. 3 is also consistent with simulations results on other systems (not yet studied experimentally) as summarized in Ref. 19 and with the theories of surface mobility.[2,3,21,45] The value $D_0 = 10^{-8}$ m^2/s corresponds to the dynamic state at which the

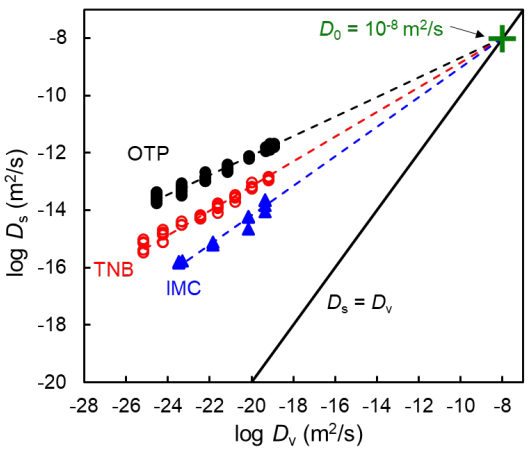

Figure 6. D_s plotted against D_v for 3 systems for which both properties have been measured. The power law $D_s = D_v^{\,x}\, D_0^{1-x}$ holds for each system, where $D_0 \approx 10^{-8}$ m^2/s corresponds to the high-temperature condition at which $D_s = D_v$. The exponent x is 0.34 for OTP, 0.43 for TNB, and 0.51 for IMC.

structural relaxation time is approximately 10 ps (calculated from $\tau = d^2/(6\,D)$, where $d \approx 0.8$ nm to represent the size of OTP, TNB, and IMC). This value is comparable to the theoretically predicted conditions under which surface and bulk mobility are equal: $\tau_\alpha = 1$ ps (Ref. 2), 1 – 10 ps (Ref. 22), 2 ps (Ref. 45). Empirically, the D_0 value of 10^{-8} m^2/s is lower than the typical gas-phase diffusivity (10^{-5} m^2/s)[46] and without invoking deep interpretation, comparable to the diffusivity at the critical point at which the distinction vanishes between liquid and vapor.[47,48]

Eq. 3 can be rearranged to read: $\log D_s(T) = \log D_v(T) + [\log D_0 - \log D_v(T)](1 - x)$, and comparison with eq. 2 yields:

$$A(T) = \log D_0 - \log D_v(T) \qquad (4)$$

$$\exp(-z/\xi) = 1 - x \qquad (5)$$

Combining eqs. 2, 4, and 5, we obtain:

$$\log D_s(T) = \log D_v(T) + [\log D_0 - \log D_v(T)] \exp(-z/\xi) \qquad (6)$$

Eq. 6 allows calculation of D_s at any temperature T from the D_v value at that temperature, the molecule-dependent penetration depth z, and the characteristic length for the mobility gradient ξ. The validity of eq. 6 depends on the validity of eqs. 2 and 3. We now test the ability of eq. 6 to describe the temperature dependence of the measured D_s values. For the systems whose D_v values are known (OTP, TNB, and IMC), the only adjustable parameter in eq. 6 is ξ. We optimize ξ for each system to best fit the measured D_s. Figure 7a compares the measured and fitted D_s values. We find an excellent agreement between the two. From the fits, we obtain ξ = 1.7 nm for OTP, 1.5 nm for TNB, and 1.3 nm for IMC. These values are reasonably close, consistent with the notion that the three systems share a similar mobility gradient. For PS1100 and PS1700, D_v has not been measured but is known at an adjacent molecular weight (1900 g/mole).[38] We estimate the D_v of PS1100 and PS1700 from that of PS1900 by T_g scaling and then perform the same test of eq. 6 as described above. The results are included in Figure 7a. Again, the measured D_s values agree well with the fitted values, yielding ξ = 1.4 nm for PS1100 and 1.5 nm for PS1700. Finally, for the systems whose D_v has not been measured, we use an approximation inspired by the clustering of the D_v values when plotted against T_g/T (Figure 4):

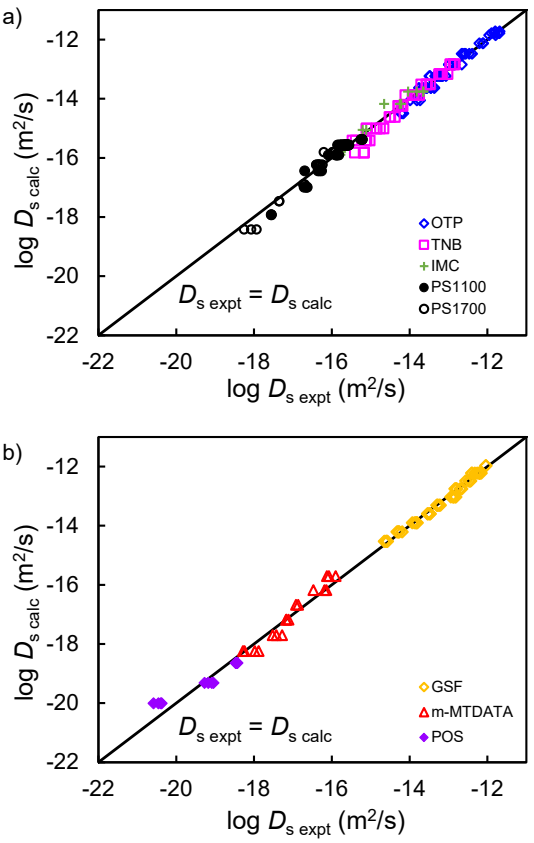

Figure 7. Comparison of measured surface diffusivity, $D_{s,expt}$ and the value $D_{s,calc}$ calculated from eq. 6 for the systems whose D_v is known (a) and unknown (b). For (b), a generic D_v is assumed (eq. 7). In both cases, ξ has been adjusted to best fit the observed D_s.

$$\log D_v(T) = \log D_v(T_g) + m_D(1 - T_g/T) \qquad (7)$$

Eq. 7 is intended to describe the D_v value near T_g where m_D is a fragility index for diffusivity, in analogy to the commonly used m index for viscosity. From a joint fit of the data on OTP, TNB, IMC, and PS1900 for $T < 1.05\ T_g$, we obtain $D_v(T_g) = 10^{-20}$ m^2/s and m_D = 53. Eq. 7 reproduces the measured D_v values for the 4 systems with a standard deviation of 0.3 decade. Using eq. 7, we perform the same test above for GSF, POS and MTDATA and the results are shown in Figure 7b. We observe a good agreement between

measured and calculated D_s values and obtain ξ = 1.7 nm for GSF, 1.4 nm for POS, and 1.6 nm for MTDATA. These values are all consistent with those obtained for other systems.

Table 1. Parameters for surface and bulk diffusion in molecular glasses.

	M (g/mol)	T_g (K)	d (nm) [a]	z (nm)	x	ξ (nm)	m_D	log $D_{v,g}$ (m^2/s)
OTP	230.3	246	0.70	0.70	0.34	1.7	48.7	-19.5
TNB	456.6	347	0.87	0.87	0.43	1.5	55.4	-20.2
IMC	357.8	315	0.76	0.89[b]	0.51	1.3	52.0	-19.9
PS1110	990	307	1.17	1.10	0.55[c]	1.4	55.7	-20.8
PS1700	1600	319	1.37	1.39	0.60[c]	1.5	55.7	-20.8
GSF	352.8	361	0.76	0.76	-	1.7	53[d]	-20[e]
MTDATA	789.2	350	1.03	1.56	-	1.6	53[d]	-20[e]
POS	700.8	331	0.97	2.18	-	1.4	53[d]	-20[e]

[a] d is the molecular size calculated from $d = \Omega^{1/3}$, where Ω is the molecular volume (molar volume/Avogadro's number). All values are from Ref. 20 except for that for MTDATA, which is given above (Ω = 1.09 nm^3) to obtain Figure 3b.
[b] Enlarged slightly from d to reflect hydrogen bonding.[19]
[c] D_v used for fitting (eq. 3) is calculated from the data on PS1900 (Ref. 38) by T_g scaling.
[e] Fixed at typical value for molecular glasses.

The success of eq. 6 to describe known D_s results using a similar set of parameters suggests a possibility to predict the surface diffusion rate for any molecular glass. For this purpose, we use eq. 6 to predict the D_s for all van der Waals molecular glasses whose D_s has been measured, with $D_0 = 10^{-8}$ m^2/s and ξ = 1.5 nm. We use eq. 7 to calculate the D_v values for all the systems (setting aside the experimentally measured D_v values), with D_v (T_g) ≈ 10^{-20} m^2/s and m_D = 53. The results are shown in Figure 8, without distinguishing the individual systems. We see a reasonably good agreement between predicted and experimental values with a standard deviation of 0.6 decade. Given the overall span of the D_s data over 9 orders of magnitude, the preliminary success is encouraging. One source of error for this model is the accuracy of eq. 7 to describe bulk diffusion (the standard deviation already amounts to 0.3 decade for the training set). The additional error comes from the slight system-to-

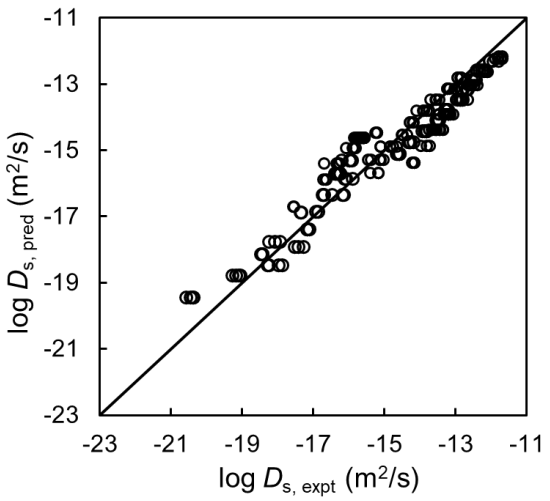

Figure 8. Comparison of measured and predicted surface diffusivity, $D_{s,expt.}$ and $D_{s,pred.}$ Eqs. 6 and 7 are used for this prediction with ξ = 1.5 nm, $D_0 = 10^{-8}$ m^2/s, D_v (T_g) = 10^{-20} m^2/s, and m_D = 53.

system variation of the ξ value (Table 1). Nevertheless, this model and its refinement have the potential to predict the surface diffusion rate in any non-hydrogen-bonded molecular glass from nothing more than its molecular structure.

Although this work was conducted to understand surface diffusion in glasses, the results provide information on the near-surface mobility gradient, a topic of significant current interest.[21,49] Below we discuss our two key conclusions and relate them to the literature: (1) the power-law relation between surface and bulk mobility (eq. 3) and (2) a generic surface mobility gradient with a double exponential dependence on depth z.

Eq. 3 is an empirical formula that describes the experimental data on three systems (OTP, TNB, and IMC; Figure 6). For each system, eq. 3 describes the relationship between the surface and bulk diffusivity, D_s and D_v, measured over a range of temperature. The three systems show different degrees of decoupling between D_s and D_v (different x) but have a similar high-mobility state ($D_0 \approx 10^{-8}$ m^2/s) at which $D_s = D_v$. We now show that eq. 3 is consistent with an equation based on the simulation results of Diaz-Vela et al.[50] and augmented later:[21]

$$\tau\,(T, z) = \tau_\alpha\,(T)^{\,1-\varepsilon(z)}\,\tau^{*\,\varepsilon(z)} \qquad (8)$$

where $\tau\,(T, z)$ is the depth (z)-dependent structural relaxation time, $\tau_\alpha\,(T)$ is the bulk structural relaxation time, $\varepsilon(z)$ is a decoupling index between 0 and 1, and $\tau^* = 1 - 10$ ps.[21] ε characterizes the degree to which $\tau\,(T, z)$ decouples from $\tau_\alpha\,(T)$ with $\varepsilon \approx 1$ signifying large decoupling that occurs near the top of the surface and 0 for no decoupling deep in the bulk. Diaz-Vela et al. showed that at low enough bulk mobility ($\tau_\alpha >> \tau^*$), ε is weakly dependent on temperature and a function of z only.

If we assume a surface molecule's penetration depth into the bulk is weakly dependent on temperature, its bottom position z in the surface mobility gradient is nearly constant. Assuming the molecule's lateral mobility (surface diffusion) is limited by the mobility of its deepest part, we obtain

$$\tau_s\,(T) = \tau_\alpha\,(T)^{\,1-\varepsilon}\,\tau^{*\,\varepsilon} \qquad (9)$$

where τ_s is the surface relaxation time. (z is dropped in eq. 9 as it is nearly constant for a given molecule.) Eq. 9 leads to eq. 3 if we assume $D \propto \tau^{-1}$. The constant x in eq. 3 is related to ε in eq. 9 by: $x = 1 - \varepsilon$. For consistency, D_0 in eq. 3 should correspond to τ^* in eq. 9, both describing the dynamic state at which surface and bulk mobility are equal. To test this, we recall the earlier result that $D_0 = 10^{-8}$ m^2/s corresponds to $\tau \approx 10$ ps for $d \approx 0.8$ nm, which is close to $\tau^* = 1 - 10$ ps.[21] We view this coherent picture as an experimental support for Eq. 8, a simulation-based result.

We now turn to the features of the surface mobility gradient inferred from our study of surface diffusion rates. For non-hydrogen-bonding glass-forming molecular liquids, our results suggest a generic surface mobility gradient of the form:

$$\log D\,(T, z) = \log D_v\,(T) + A(T) \exp\,(-\,z\,/\,\xi) \qquad (10)$$

where $D\,(T, z)$ is the depth-dependent local diffusivity, and all other parameters have been defined above. Note that eq. 10 is different from eq. 2 in that it describes the *variation of mobility with depth z*, while eq. 2 describes how the *overall* surface diffusion rate D_s depends on the depth of penetration (for a given system the penetration depth is fixed; see Table 1). We justify eq. 10 on the basis that (1) eq. 2 accurately describes our D_s results (Figures 7 and 8) and (2) each observed D_s presumably reports the mobility at the bottom of a surface molecule. Based on this work, the parameters in eq. 10 are: $\xi \approx 1.5$ nm; $A\,(T) = \log D_0 - \log D_v(T)$, where $D_0 \approx 10^{-8}$ m^2/s. At the DSC T_g, $A\,(T_g) \approx 12$.

Given that a double-exponential profile of the surface mobility gradient has been proposed based on simulation results and theoretical analysis, we view its ability to describe our results as an experimental support for this profile. Our finding of $\xi \approx 1.5$ nm for non-hydrogen-bonding molecular liquids is in reasonable agreement the simulation and theoretical results ($\xi = 2$–$3\ d$, where d is bead diameter).[21,42] It is noteworthy, however, that the values from simulations and theory are often reported to scale with the molecular size d. Our values (Table 1) do not appear to show such scaling behavior. As for the amplitude A in eq. 10, the simulations summarized in Ref. 21 indicate $A = 2$–4, obtained for systems of higher mobility ($\tau_\alpha \sim 1$ ns) than the experimental systems. Using 1 ns for τ_α and our expression for $A(T)$ in eq. 10, we estimate $A\,(T) \approx 2$, in fair agreement with the simulation results. Based on the ECNLE theory, Phan and Schweizer obtain $A\,(T_g) = 12$ for hard spheres and 11–17 for real polymers mapped onto the model,

where T_g is the temperature at which τ_α = 100 s (close to the value at the DSC T_g, ~10 s).[42] Overall, there is encouraging agreement between simulations, theory, and experiment on the double-exponential profile for the surface mobility gradient, while the details of the gradient and its system dependence awaits future clarification.

Conclusions

In this work, we have applied the method of surface grating decay to measure the surface diffusion in the glass of a discotic organic semiconductor, MTDATA. The high-temperature decay occurs by viscous flow and the low-temperature decay by surface diffusion (Figures 2 and 3). The surface diffusion of MTDATA is enhanced relative to the bulk rate by 4 orders of magnitude at T_g (Figure 4). The MTDATA result joins the previously observed trend between surface diffusivity and penetration depth (Figure 5). This argues for a generic surface mobility gradient for non-hydrogen-bonded molecular glasses with a double-exponential decrease of mobility with depth (eq. 2). The power-law relation between surface and bulk diffusivity (eq. 3) provides access to the parameters characterizing the double-exponential mobility gradient, leading to an equation (eq. 6) useful for fitting (Figure 7) and predicting (Figure 8) the surface diffusion coefficient. This model has the potential to predict surface diffusion in molecular glasses from the molecular structure alone. This ability is relevant for predicting surface crystallization rates. As systems with large surface diffusion coefficients often produce highly stable glasses via PVD, this model also provides a route to improve device stability and performance.

Under the assumption that surface diffusion is limited by the mobility at the deepest anchoring point of surface molecules, our results can be used to provide a depth profile of near-surface mobility. Our results support the recently proposed double-exponential form for the surface mobility gradient and give a quantitative description of this gradient in terms of diffusivity (eq. 10) with $D_0 \approx 10^{-8}$ m^2/s and $\xi \approx 1.5$ nm. It is intriguing that despite the different molecular weights and shapes of the systems investigated, they all appear to have a similar surface mobility gradient. This finding can be further examined by simulations where molecular size and geometry are systematically varied to test the robustness of a generic mobility gradient. While this work has focused on non-hydrogen-bonding molecular glasses, how the introduction of hydrogen bonds affects the mobility gradient deserves future investigation.

Conflicts of interest

There are no conflicts of interest to declare.

Acknowledgements

This research was primarily supported by NSF through the University of Wisconsin Materials Research Science and Engineering Center (Grant DMR-1720415). We thank Kushal Bagchi for helpful conversations.

References

[1] L. Zhu, C. W. Brian, S. F. Swallen, P. T. Straus, M. D. Ediger, and L. Yu, Phys. Rev. Lett. **106**, 256103 (2011).
[2] J. D. Stevenson, and P. G. Wolynes, J. Chem. Phys. **129,** 234514 (2008).
[3] S. Mirigian, and K. S. Schweizer, J. Chem. Phys. **143**, 244705 (2015).
[4] Y. Sun, L. Zhu, K. L. Kearns, M.D. Ediger and L. Yu, Proc. Natl. Acad. Sci. **108**, 5990 (2011).
[5] T. Wu, and L. Yu, Pharm. Res. **23**, 2350 (2006).
[6] M. D. Ediger, J. Chem. Phys. **147**(21), 210901 (2017).
[7] A. N. Raegen, J. Yin, Q. Zhou, and J. A. Forrest, Nat. Mat. **19**(10), 1110-1113 (2020).
[8] K. Yoshimoto, T. S. Jain, P. F. Nealey, and J. J. De Pablo, J. Chem. Phys. **122**(14), 144712 (2005).
[9] S. P. Delcambre, R. A. Riggleman, J. J. de Pablo, and P. F. Nealey, Soft Matter **6**(11), 2475-2483 (2010).
[10] X. Li, X. Liang, Z. Zhang, J. Ma, and J. Shen, Scripta Materialia **185**, 100-104 (2020).
[11] Y. Shirota, T. Kobata, and N. Noma, Chem. Lett. **18**(7), 1145-1148 (1989).
[12] Y. Kuwabara, H. Ogawa, H. Inada, N. Noma, and Shirota, Y. Adv. Mater. **6**(9), 677-679 (1994).
[13] Y. Shirota, J. Mater. Chem. **15**(1), 75-93 (2005).
[14] C. W. Tang, and S. A. VanSlyke, Appl. Phys. Lett. **51**(12), 913-915 (1987).
[15] K. Bagchi, M. E. Fiori, C. Bishop, M. F. Toney, and M. D. Ediger, J. Phys. Chem. B **125**(1), 461-466 (2020).
[16] K. Bagchi, and M. D. Ediger, J. Phys. Chem. Lett. **11**(17), 6935-6945 (2020).
[17] S. F. Swallen, K. L. Kearns, M. K. Mapes, Y. S. Kim, R. J. McMahon, M. D. Ediger, T. Wu, L. Yu, and S. Satija, Science **315**(5810), 353-356 (2007).
[18] M. D. Ediger, J. de Pablo, and L. Yu, Acc. Chem. Res. **52**(2), 407-41 (2019).
[19] Y. Chen, W. Zhang, and L. Yu, J. Phys. Chem. B **120**, 8007-8015 (2016).
[20] Y. Li, W. Zhang, C. Bishop, C. Huang, M.D. Ediger, and L. Yu, Soft. Matt. **16**, 5062-5070 (2020).
[21] K. S. Schweizer, and D. S. Simmons, J. Chem. Phys. **151**, 240901 (2019).
[22] P. Scheidler, W. Kob and K. Binder, Europhysics Letters (EPL) **59**(5), 701-707 (2002).
[23] H. J. Werner, P. J. Knowles, G. Knizia, F. R. Manby, and M. Schütz, Mol. Sci. **2**, 242−253 (2012).
[24] A. H. Larsen, J. J. Mortensen, J. Blomqvist, I. E. Castelli, R. Christensen, M. Dułak, J. Friis, M. N. Groves, B. Hammer, C. Hargus, et al. J. Phys.: Condens. Matter **29**, 273002 (2017).
[25] J. P. Perdew, K. Burke, and M. Ernzerhof, Phys. Rev. Lett. **77**, 3865−3868 (1996).
[26] S. Grimme, J. Antony, S. Ehrlich, and H. Krieg, J. Chem. Phys. **132**, 154104 (2010).
[27] T. H. Dunning, J. Chem. Phys. **90**, 1007−1023 (1989).
[28] W.W. Mullins, J. Appl. Phys. **30**, 77 (1959).
[29] L. M. Martinez, and C. A. Angell, Nature **410**, 663-667 (2001).
[30] D. J. Plazek, C. A. Bero, and I. C. Chay, J. Non-Cryst. Solids **172**, 181−190 (1994).
[31] D. J. Plazek, and J. H. Magill, J. Chem. Phys. **45**, 3038−3050 (1966).
[32] W. Zhang, C. W. Brian, and L. Yu, J. Phys. Chem. B **119**, 5071 (2015).

[33] S. Ruan, W. Zhang, Y. Sun, M. D. Ediger, and L. Yu, J. Chem. Phys. **145**, 064503 (2016).
[34] W. Zhang, and L. Yu, Macromolecules. **49**, 731 (2016).
[35] M. K. Mapes, and S. F. Swallen, and M. D. Ediger, J. Phys. Chem. B **110**, 507 (2006).
[36] S. F. Swallen, K. Traynor, R. J. McMahon, M. D. Ediger, and T. E. Mates, J. Phys. Chem. B **113**, 4600 (2009).
[37] S. F. Swallen, and M. D. Ediger, Soft Matter **7**, 10339 (2011).
[38] O. Urakawa, S. F. Swallen, M. D. Ediger, and E. D. von Meerwall, Macromolecules **37**, 1558 (2004).
[39] D. M. Walters, L. Antony, J. J. de Pablo, and M. D. Ediger, J. Phys. Chem. Lett. **8**(14), 3380-3386 (2017).
[40] A. Gujral, J. Gomez, S. Ruan, M. F. Toney, H. Bock, L. Yu, and M. D. Ediger, Chem. Mater. **29**(21), 9110-9119 (2017).
[41] T. J. Ferron, J. L. Thelen, K. Bagchi, C. Deng, E. Gann, J. J. de Pablo, M. D. Ediger, D. F. Sunday, and D. M. DeLongchamp, ACS Appl. Mater. Interfaces, In Press.
[42] A. D. Phan, K.S. Schweizer, J. Chem. Phys. **150**, 044508 (2019).
[43] A. D. Phan, and K. S. Schweizer, Macromolecules, **52**, 5192 (2019).
[44] Y. Li, A. Annamareddy, D. Morgan, Z. Yu, B. Wang, C. R. Cao, J. H. Perepezko, M. D. Ediger, P. M. Voyles and L. Yu, Phys. Rev. Lett. Accepted.
[45] S. Capaccioli, K. L. Ngai, M. Paluch, and D. Prevosto, Phys. Rev. E **86**, 051503 (2012).
[46] D. Jakubczyk et al., J. Phys. Chem. A 114, 3483 (2010).
[47] H. Hamann, C. Hoheisel, and H. Richtering, Phys. Chem. **76**(3-4), 249-253 (1972).
[48] T. Saitoh, N. Yoshio, and S. Shigezo, Bull. Chem. Soc. Jpn. **65**, 3480-3481 (1992).
[49] A. Ghanekarade, A. D. Phan, K. S. Schweizer, and K. S. Simmons, Proc. Natl. Acad. Sci. **118**(31), (2021).
[50] D. Diaz-Vela, J.-H. Hung, and D. S. Simmons, ACS Macro Lett. **7**, 1295 (2018).